Size-selective growth of double-walled carbon nanotube forests from engineered iron catalysts

TAKEO YAMADA[1], TATSUNORI NAMAI[1], KENJI HATA[1]*, DON N. FUTABA[1], KOHEI MIZUNO[1], JING FAN[2], MASAKO YUDASAKA[2,3], MOTOO YUMURA[1] AND SUMIO IIJIMA[1]

[1]Research Center for Advanced Carbon Materials, National Institute of Advanced Industrial Science and Technology (AIST), 1-1-1 Higashi, Tsukuba, Ibaraki 305-8565, Japan
[2]Japan Science and Technology Agency, 34 Miyukigaoka, Tsukuba, Ibaraki 305-8501, Japan
[3]NEC Corporation, 34 Miyukigaoka, Tsukuba, Ibaraki 305-8501, Japan
*e-mail: kenji-hata@aist.go.jp

Published online: 3 November 2006; doi:10.1038/nnano.2006.95

We have succeeded in synthesizing vertically aligned doubled-walled carbon nanotube (DWNT) forests with heights of up to 2.2 mm by water-assisted chemical vapour deposition (CVD). We achieved 85% selectivity of DWNTs through a semi-empirical analysis of the relationships between the tube type and mean diameter and between the mean diameter and the film thickness of sputtered Fe, which was used here as a catalyst. Accordingly, catalysts were engineered for optimum DWNT selectivity by precisely controlling the Fe film thickness. The high efficiency of water-assisted CVD enabled the synthesis of nearly catalyst-free DWNT forests with a carbon purity of 99.95%, which could be templated into organized structures from lithographically patterned catalyst islands.

Double-walled carbon nanotubes (DWNTs) are a unique form of carbon nanotubes (CNTs) composed of two coaxial single-walled carbon nanotubes (SWNTs). They therefore benefit from a synergetic blend of both SWNT and multiwalled carbon nanotube (MWNT) characteristics, exhibiting the electrical and thermal stability of MWNTs and the flexibility of SWNTs. The superior physical and field emission[1–3] properties of DWNTs are advantages for use in such applications as field-emission displays (FEDs), super-tough fibres[5] and field-effect transistors[6]. The most prominently pursued application of DWNTs is as electron emitters, because SWNTs have an unsatisfactory emission lifetime for real applications, despite having the advantage of a low threshold voltage. Conversely, MWNT emitters possess the durability for real applications, but their threshold voltage is high. Therefore, DWNTs are the best choice for real FED applications because they possess the advantages of both SWNT and MWNT emitters, that is, low threshold voltage and high durability. To date, DWNTs with size in the range 2–5 nm have been successfully used in FEDs[4].

Hafner and co-workers first synthesized DWNTs[7] by catalytic CVD[8–17]. Following this pioneering work, a number of researchers have reported the successful synthesis of DWNTs[8–23], using the arc-discharge method[18–20], coalescence of C_{60} peapods[21] and floating catalyst CVD[22,23]. Despite all of these efforts, highly efficient and selective growth of DWNTs remains a challenge.

Recently, the introduction of a small and controlled amount of water into the growth environment of standard CVD (hereafter denoted supergrowth) was reported to increase the synthesis efficiency of SWNTs to unprecedented levels[24–26]. In this paper, we report the synthesis of catalyst-free DWNT forests with millimetre-scale height by water-assisted CVD from catalyst nanoparticles tailored to achieve maximum DWNT selectivity. Here, catalyst engineering was the key factor for selective DWNT synthesis. We determined the optimum mean tube diameter for selective DWNT synthesis and grew CNTs with this optimum mean diameter by precisely controlling the thickness of the Fe catalyst film. The carbon purity was over 99.95 wt%, and we could pattern the growth of vertically aligned CNT forests into organized structures of desired shape from lithographically patterned catalyst islands. Our results represent a breakthrough in the synthesis of highly pure, efficient and scalable DWNTs, enabling the immediate use of the as-grown material without purification, consequently opening up opportunities for this promising but rather unexplored CNT. Finally, we present our preliminary results, which show that a small difference in the catalyst metal film can induce a significant difference in the DWNT diameter, a result that may open up a route towards the diameter-controlled synthesis of DWNTs.

RESULTS AND DISCUSSION

To understand and control CNT synthesis, we first studied the relationship between tube type and diameter by constructing a phase diagram (Fig. 1a) of the relative populations of SWNTs, DWNTs and MWNTs versus the tube diameter from the analysis of 1,432 CNTs with diameters ranging from 1.0 to 5.0 nm using transmission electron microscopy (TEM). The CNTs were grown from thin Fe catalytic films (0.8–1.9 nm thick) made using sputter target (1) (see Methods). The phase diagram highlights an empirically well-known fact that the number of graphitic walls in a CNT strongly depends on the CNT diameter, where small tubes

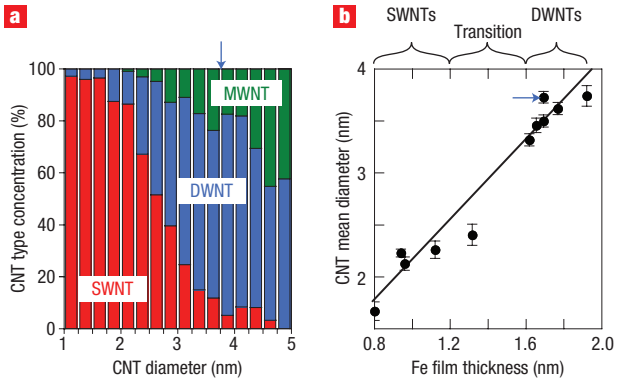

Figure 1 Trends in CNT type and diameter. a, Phase diagram of the relative concentrations of SWNTs (red), DWNTs (blue) and MWNTs (green) as a function of the CNT diameter, obtained from 1432 CNTs. **b**, Plot of CNT mean diameter as a function of Fe film thickness. The analysed CNTs for both **a** and **b** were prepared using Fe film catalysts from sputter target (1). The blue arrows indicate the point of maximum selectivity of DWNTs.

have a strong tendency to be SWNTs, and larger tubes tend to be DWNTs or MWNTs. This is evidenced in the well-known fact[27–29] that a very thin layer of metal film (typically around 1 nm), which produces small CNTs, is necessary to grow SWNTs selectively. More importantly, the phase diagram provides quantitative insight into the relationship between CNT diameter and the number of walls, which serves as the key factor in achieving selective DWNT synthesis. The phase diagram shows that DWNTs occupy the majority of the nanotube population within a distinct diameter range, 3.0–4.5 nm, sandwiched between the SWNT and MWNT regions and with a maximum DWNT selectivity occurring when the mean CNT diameter is around 3.75 nm (blue arrows in Fig. 1a, b). Selective DWNT growth is achieved by tuning the tube diameter within this DWNT region.

In addition, we found that the mean CNT diameter can be precisely tuned by controlling the thickness of the Fe thin film. Empirically, it is well established that a thin catalytic metal film (around 1 nm) is required to grow SWNTs, and thicker metal films (10 nm, for example) are necessary for MWNT growth. It is generally believed that thin (thick) metal films break up into smaller (larger) catalytic nanoparticles, which, in turn, produce smaller (larger) tubes. To seek more precise size control, we quantitatively investigated the relationship between the thickness of the catalytic Fe thin film and mean CNT diameter. Eleven independent batches of CNTs were grown from Fe thin films with thicknesses ranging from 0.8 nm to 1.9 nm. For each batch, a diameter distribution histogram of the CNTs was generated from TEM images, fitted to a gaussian curve and the mean CNT diameter of the batch was estimated. From such analyses, the mean CNT diameter was found to increase approximately linearly with Fe thin film thickness (Fig. 1b). This important finding has made it possible for us to accurately control the mean CNT diameter within the DWNT region.

We combined these results to demonstrate the application of our approach for selective syntheses of DWNTs and SWNTs. Figure 2a shows a set of histograms of the type and diameter of CNTs synthesized from Fe films tuned to synthesize SWNTs (Fe thickness: 0.8–1.2 nm) and DWNTs (Fe thickness: 1.6–1.9 nm), respectively. Figure 2a shows that it is possible to control the selectivity of SWNTs and DWNTs with high reproducibility corresponding to the prediction of the phase diagram.

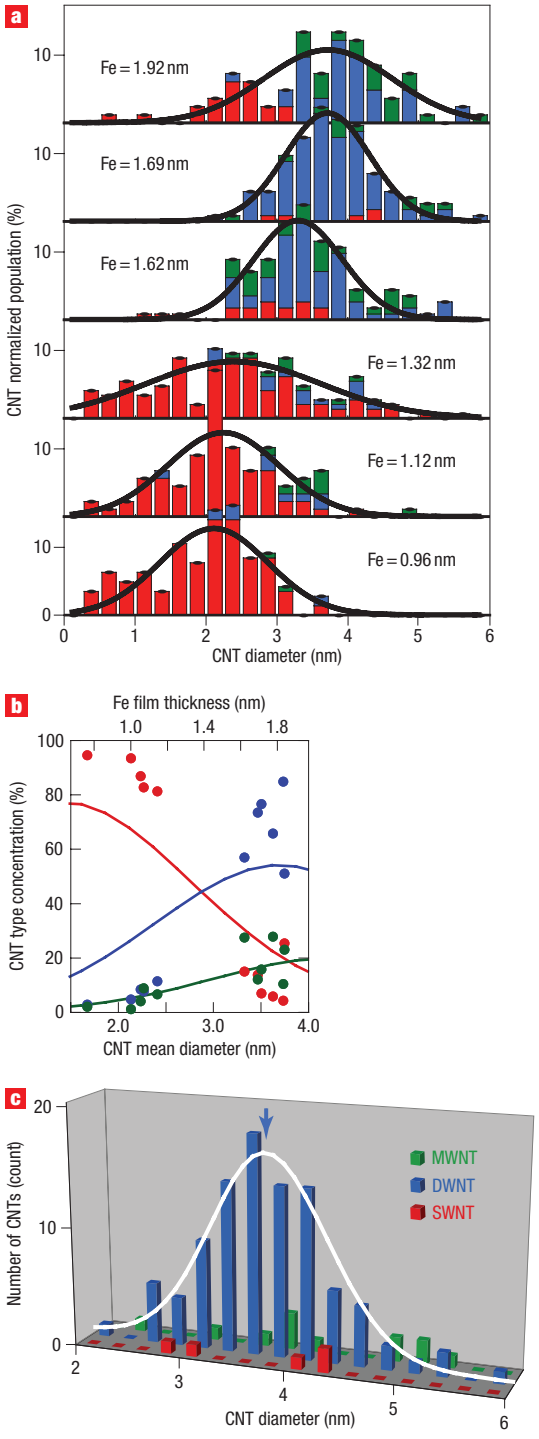

Figure 2 Selective synthesis. a, A family of histograms of the type and diameter of CNTs synthesized from 0.96, 1.12, 1.32, 1.62, 1.69 and 1.92 nm Fe thin films with gaussian fitting (solid line). Red, blue and green bars denote SWNTs, DWNTs and MWNTs, respectively. **b**, Plot of the calculated existence ratios (lines) and the experimental existence ratios (solid circles) for SWNTs (red), DWNTs (blue) and MWNTs (green) as a function of CNT mean diameter and Fe film thickness. **c**, Plots of the population distribution of the maximum DWNT (blue) selectivity (85% DWNT) with SWNT (red) and MWNT (green) population distributions as a function of diameter for a 1.69-nm Fe thin film with gaussian fitting for the DWNT distribution (white line). The blue arrow indicates the mean diameter for maximum DWNT selectivity. All CNTs for this figure were prepared using Fe film catalysts from sputter target (1).

A transition region existed (Fe thickness: 1.2–1.6 nm) between the SWNT and DWNT regions where growth showed less controllability. Here, a noticeable fluctuation existed in the type of CNTs and mean CNT diameter for CNTs synthesized from different batches of Fe films with the same thickness. Moreover, CNTs grown from films in this region frequently exhibited a relatively broad diameter distribution (see the CNT histogram for a film of 1.32 nm thickness in Fig. 2a). In contrast, for CVD growths carried out in the SWNT and DWNT regions, the diameter histograms had a similar and relatively sharper full-width at half-maximum (FWHM) of 1.9 nm.

To further investigate which factors determine the number of walls in the CNTs, we calculated the existence ratios of SWNTs, DWNTs and MWNTs as a function of the mean CNT diameter from the phase diagram of Fig. 1a. We estimated the diameter distribution for each nanotube type by assuming it followed a gaussian distribution with an FWHM of 1.9 nm. The calculated (estimated) existence ratios are shown as lines in Fig. 2b and can be directly compared with the experimental existence ratios, which are plotted as solid circles. Interestingly, the experimentally obtained selectivities of SWNTs and DWNTs were higher than those estimated by calculation in most cases. This provides evidence that when the catalytic film is tuned in thickness for SWNT synthesis, CNTs within the transition region have a tendency to become SWNTs, regardless of their diameter, and when the film is tuned for DWNT synthesis, they have a tendency to become DWNTs. Additionally, we observed that fluctuation from batch to batch in DWNT selectivity is more sensitive than that predicted from the calculations. These experimental results suggest that there is an additional factor playing an important role in determining the number of walls for a CNT.

The maximum DWNT selectivity achieved using our approach was 85%, as shown in the DWNT (and SWNT, MWNT) diameter and population distribution for samples grown using the 1.69 nm film (Fig. 2c). This DWNT selectivity is one of the highest reported, and it is worth noting that it was achieved on an as-grown sample without any additional processes implemented to improve selectivity[14–17,22,23]. The maximum DWNT selectivity was achieved when the Fe thin film thickness was 1.69 nm, from which DWNTs with an average diameter of 3.7 nm were synthesized. These results correspond well with our estimation deduced from the phase diagram and the dependence of mean CNT diameter on Fe thickness, highlighting the controllability of our approach.

Water-assisted CVD was implemented to demonstrate highly efficient DWNT syntheses from these engineered catalysts. Similar to the case for SWNTs, water-assisted CVD resulted in massive growth of DWNTs that self-organize into vertically aligned DWNT forests of millimetre-scale height. Our best result to date is a DWNT forest 2.2 mm in height on a 20 × 20 mm Si substrate (Fig. 3a). A possible mechanism for nanotube growth termination is oxidization of the catalyst. Furthermore, we observed a dependence of our ability to grow CNT forests on catalyst layer thickness. We discovered a threshold in the thickness (0.8 nm) below which we were unable to grow forests. However, within the DWNT region the forest height showed very little dependence on the Fe thin film thickness. Close examination (Fig. 3b) at the edge of the DWNT forest by scanning electron microscopy (SEM) reveals densely packed and vertically aligned DWNTs. High-resolution TEM images (Fig. 3c; see Supplementary Information, Fig. S1) show only clean nanotubes, which are mainly DWNTs in the form of small bundles. Medium-scale wide-view TEM images are provided as a broad assessment of the general quality of our DWNTs (see Supplementary Information). Low-resolution TEM images (Fig. 3d) of the as-grown forest further reveal the absence of dark spots that would indicate the presence of metallic particles and supporting materials that usually comprise a major constituent of as-grown material. Additionally, TEM images show that the difference between the radii of the inner tubes and outer tubes is close to the spacing of graphite layers.

To provide a quantitative assessment of the quality of the DWNTs, we implemented characterization by macro Raman spectroscopy (sampling area ~1 mm^2) on 12 samples synthesized from 12 independent CVD growths. The average Raman spectrum of the DWNT forests (Fig. 3e) excited by 532-nm wavelength shows a strong G-band intensity, originating from the C–C stretching mode at ~1,590 cm^{-1}, compared to the D-band intensity, associated with defects and amorphous carbon at ~1,340 cm^{-1}, indicating a reasonable quality of the DWNTs (the ratio between G-band and D-band intensities, the G/D ratio, is 5.2). Although the D-band could be due to carbon impurities in the samples, we believe that it is more likely that it originates from defects in the tubes (see Supplementary Information, Fig. 1). Other reported G/D ratios of DWNTs are in the range 3.5–40 for DWNTs synthesized by CVD[8,10,12–17], 4.8–7 for DWNTs synthesized by arc discharge[18,20], 17–40 for DWNTs synthesized using floating catalyst[22,23], and around 200 for DWNTs synthesized by annealing peapods[21]. We believe that the feasibility of synthesizing DWNTs using our approach for applications is not hindered by the quality of the DWNTs as estimated by the G/D ratio, because Raman spectroscopy alone does not comprise a complete assessment of DWNTs for real applications. Furthermore, although the G/D ratio is the weakest numerical evaluation of water-assisted CVD, other factors, such as carbon purity, length and alignment (where this material is extraordinarily superior[9,17–19]) are also very important[30]. Moreover, the G/D ratio (see Supplementary Information, Fig. 2) can be increased to 20 by decreasing the growth rate, a result that indicates that the quality of DWNTs could be tuned to meet the quality requirement of a specific application.

Thermo-gravimetric analysis (TGA) on 0.96 mg of the as-grown material (Fig. 3f) showed no measurable residue remaining above 750 °C, indicating very high purity. The combustion range of the DWNTs was 550–740 °C, with a peak weight reduction at 700 °C. Furthermore, quantitative elemental analysis with X-ray fluorescence spectrometry only detected the presence of 0.053 wt% Fe impurity suggesting a carbon purity over 99.95 wt%. The exceptionally high purity of this DWNT enables use of the as-grown material without purification, representing a significant advantage of this approach because purification processes are well known to damage nanotubes. It remains an open question whether high-quality DWNTs with high G/D ratio that require purification before use are, in fact, superior to reasonable-quality DWNTs that can be used without any purification.

Realization of large-scale organized SWNT structures of desired shape and form is important for obtaining scaled-up functional devices. For MWNTs, successful fabrication of organized structures has been demonstrated, although it remains to be seen if similar structures could be made from DWNTs. Significantly, with the assistance of water, DWNTs grow easily from lithographically patterned catalyst islands into well-defined vertical-standing organized structures, as demonstrated by the large-scale arrays of macroscopic rectangular parallelepipeds that can be obtained (Fig. 3g–j) with 150-μm width, 250-μm pitch and a height close to 500 μm. Growth on patterned samples usually results in less efficient growth compared to bulk growth. The growth efficiency strongly depends not only on the size of the patterns but also on their separations.

Finally, we demonstrate that subtle differences in catalytic films of the same thickness can cause a considerable difference in the phase diagram in Fig. 1a, confirming the extreme sensitivity of

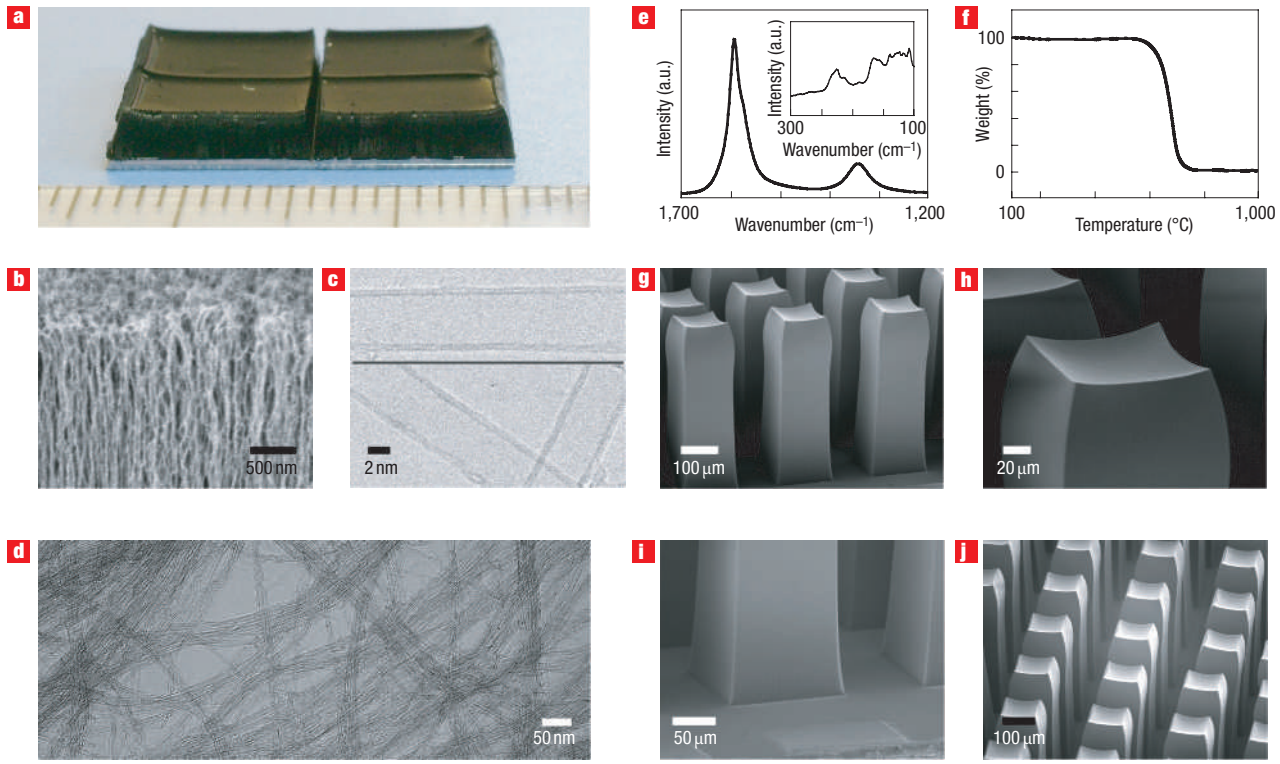

Figure 3 Highly efficient DWNT synthesis. **a**, 20 × 20 mm vertically standing DWNT forest of 2.2 mm height grown using a 1.69 nm Fe film. The scale along the bottom is marked in mm. **b**, SEM image of the edge of the DWNT forest shown in **a**. **c**, High-resolution TEM image verifying the presence of DWNTs and the absence of amorphous carbon and metal particles. **d**, Low-resolution TEM image of the DWNTs showing the absence of metallic particles and support materials. **e**, Raman spectra with distinct radial breathing mode peaks (inset). **f**, TGA plot of the weight as a function of temperature. **g–j**, SEM images of the designed macroscopic rectangular parallelepipeds of DWNTs: expansive view from side (**g**); magnified view from the top (**h**); magnified view from the base (**i**); expansive view from the top (**j**). CNTs in this figure were grown using Fe film catalysts from sputter target (1).

the number of CNT walls on the catalyst. Taking advantage of this phenomenon enabled us to synthesize DWNT ensembles with different mean diameters. To illustrate this, we constructed another phase diagram of the relative populations of SWNTs, DWNTs and MWNTs from CNTs grown from a different sputter target (2) (See Methods) with identical CVD growth conditions (Fig. 4a). When compared with the phase diagram of Fig. 1a, the phase diagram is shifted along the diameter axis approximately 0.75 nm towards larger CNTs as indicated by the arrows in Fig. 4b. We used this phase diagram to guide the syntheses of DWNT (SWNT) samples with larger diameters as demonstrated by the two histograms in Fig. 4c, identifying the type and diameter of CNTs grown from two catalytic Fe films tuned in thickness to selectively grow DWNTs and SWNTs, respectively. This unique aspect extends our ability to grow a variety of CNTs and thus is useful in many practical applications. For example, in our previous researches[24], we used sputter target (2) to grow large SWNTs with mean diameters approaching 3.0 nm to maximize growth yield. In this research, we instead used sputter target (1) to grow smaller DWNTs. The results presented in this paper were repeatable with different sputter targets; that is, although targets from different suppliers showed consistently different CNT growth, they were consistent for each supplier. We carried out careful experiments to characterize the catalytic Fe thin films sputtered from targets (1) and (2) by X-ray photoelectron spectroscopy (XPS) (Fig. 4d, e), optical adsorption and electronic conductive measurements. No noticeable difference was observed between the two films by these characterizations, indicating that the origin inducing this huge difference in CNT growth stems from a minute difference in the targets. In order to provide further insights into this difficult problem, we have carried out additional characterization of the two Fe films by X-ray diffraction (XRD) (see Supplementary Information, Fig. S3), which revealed a difference in the ratio of the (110) and (211) reflection intensities. The XRD result suggests that the two Fe films have different grain structures that might be caused by a difference in impurities (see Supplementary Information, Table S1) or the grain structures of the two targets themselves. These results show how the almost undetectable difference in sputter targets can lead to a significant difference in the outcome, and we hope that this result invokes further efforts to address and fully clarify this interesting and also very important issue, which will lead to further diameter control of DWNTs and better understanding of the role of the catalyst in CNT growth.

There are a couple of possible routes to achieve improved DWNT diameter control. One route could be the use of Fe alloys as catalysts (for example, containing Co, Ni or Mo) to shift the peak in the phase diagram (Fig. 1a) and thus produce DWNTs with different diameters. Although we do not believe that the relatively large diameter of our DWNTs is a problem for important applications such as FEDs (in fact, it is likely that larger DWNTs may show superior durability due to smaller curvature effects), it is important to achieve smaller DWNTs, particularly for electronic and optical applications. Xu and

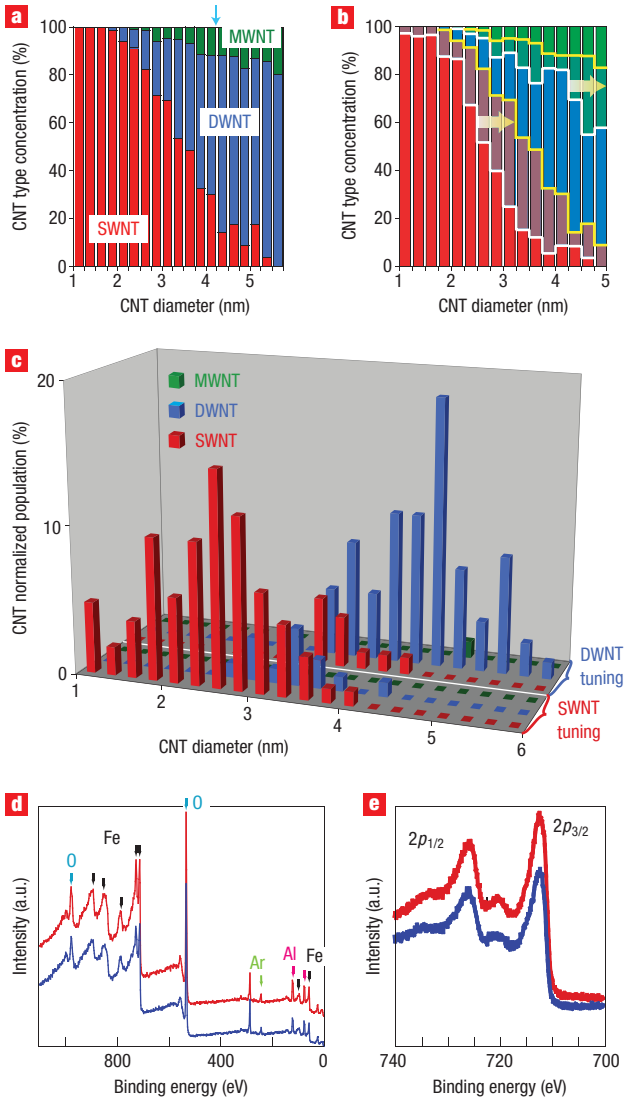

Figure 4 Sensitivity of CNT type to sputter target. a, Phase diagram of the relative concentrations of SWNTs (red), DWNTs (blue) and MWNTs (green) as a function of CNT diameter obtained from 1,330 CNTs using sputter target (2). The blue arrow indicates mean diameter for maximum DWNT selectivity. **b**, Comparison of Fig. 1a and Fig. 4a. The difference is seen as a shift towards larger diameters from Fig. 1a to Fig. 4a, as indicated by arrows from the white to yellow borders. **c**, Typical histograms tuned for SWNTs (three front histograms) and DWNTs (three rear histograms) from two Fe catalyst thicknesses using sputter target (2). Red, blue and green bars denote the normalized SWNT, DWNT and MWNT populations, respectively, in each histogram. **d**, Survey XPS spectra of prepared catalysts from Fe sputter target (1) (red line) and Fe sputter target (2) (blue line) with chemical assignment (Fe: black; O: light blue; Al: pink; Ar: light green). **e**, XPS spectra of Fe.

co-workers[31] have reported that pretreatment with radical hydrogen generated by a hot filament results in growth of SWNT forests with small nanotubes in the range 0.8–1.6 nm. These results suggest that changing the pretreatment process, particularly exposure of the catalyst to active hydrogen, may be one possible route to grow smaller DWNTs using our approach.

In conclusion, we have succeeded in achieving highly efficient synthesis of nearly catalyst-free DWNTs and DWNT forests with the assistance of water. Engineered catalysts, through precise sputtering to a semi-empirically derived thickness, were essential in achieving the selective synthesis of DWNTs and made possible the synthesis of CNT material with 85% DWNTs, one of the highest reported selectivities. Our approach has several distinct advantages over previous methods. First, this research demonstrates the first synthesis of DWNTs on flat substrates, a point that has clear advantages for direct fabrication of functional devices, such as DWNT electronic devices. Secondly, DWNT forests represent a new form of CNT material, opening up new opportunities for scientific research and development of applications such as DWNT FEDs or CNT membranes[32].

METHODS

SYNTHESIS

CNTs were grown from catalytic thin Al_2O_3 (~30 nm)/Fe metal layers sputtered on Si substrates with an oxidized layer of thickness 600 nm. Two different Fe sputter targets (1) (99.99%) and (2) (99.9%) provided from different suppliers (Mitsui Engineering & Shipbuilding for (1), and Sumitomo Metal Mining for (2)) were used. As discussed in detail in the following, sputter targets provided from the same supplier showed outstanding consistency in growth, but targets provided from different suppliers showed consistent variation. The sputtering process was carried out using a sputtering instrument equipped with a load-lock chamber dedicated to preparing catalysts. This provided a well-isolated environment to ensure reproducibility of our process because the targets were not exposed to air, and no additional impurities entered the system. As the prepared Fe thin film was around 1.0 nm and very thin, it was preferred to have a sputtering rate that was as slow (but stable) as possible. To maximize our control over sputtering levels, we minimized the sputtering rate to deposit a 1.0-nm-thick Fe film with a time exceeding 30 s. This ensures that the deposition process is both very stable and repeatable. The thickness of the Fe thin film was varied in the range 0.8–1.9 nm. When annealed to high temperatures, the Fe thin film converted into well-defined and isolated individual Fe nanoparticles that acted as catalysts for CNT synthesis[33–35]. As shown in the main text, the thickness of the Fe layer is the critical factor in achieving selective growth of DWNTs. CVD was carried out at with an ethylene carbon source (99.999%) and water as a catalyst preserver[24,25] and enhancer[26]. Water vapour was supplied by passing a portion of the helium carrier gas through a water bubbler. The water concentration was measured by a water monitor directly connected to the exhaust line. Pure helium (99.9999%) with hydrogen (99.99999%) (total flow 1,000 cm^3 per minute at standard temperature and pressure) was used as a carrier gas at 1 atm with a small and controlled amount of water vapour supplied from the water bubbler. Typical CVD growth was carried out at 750 °C with ethylene (10–150 cm^3 per minute at standard temperature and pressure) and a water concentration of 20–500 p.p.m. for 10–30 min. The optimum water–carbon balance depended significantly on experimental conditions, such as growth temperature, ethylene flow rate, catalyst and the furnace used.

Transmission electron microscopy images were taken using a JEOL JEM–2000FX instrument. Scanning electron microscopy images were taken using a Hitachi S-4800 instrument. Raman spectroscopy was performed using a Thermo-Electron Raman spectrometer with 532-nm excitation wavelength. Thermo-gravimetric analysis was carried out using a Rigaku Thermo Plus 2.

X-ray photoelectron spectroscopy measurements were carried out using Physical Electronics PHI 5800 MultiTechnique with an Al Kα X-ray source.

Received 19 June 2006; accepted 29 September 2006; published 3 November 2006.

References

1. Seko, K., Kinoshita, J. & Saito, Y. *In situ* transmission electron microscopy of field-emitting bundles of double-wall carbon nanotubes. *Jpn J. Appl. Phys.* **44,** L743–L745 (2005).
2. Wang, Y.Y. *et al.* Growth and field emission properties of small diameter carbon nanotubes films. *Diam. Relat. Mater.* **14,** 714–718 (2005).
3. Machida, H. *et al.* Improvement in field emission uniformity from screen-printed double-walled carbon nanotube paste by grinding. *Jpn J. Appl. Phys.* **45,** 1044–1046 (2006).
4. Kurachi, H. *et al.* FED with double-walled carbon nanotube emitters. *IDW Proc.* 1237–1240 (2001).
5. Zhang, M., Atkinson, K.R. & Baughman, R.H. Multifunctional carbon nanotube yarns by downsizing an ancient technology. *Science* **306,** 1358–1361 (2004).
6. Shimada, T. *et al.* Double-wall carbon nanotube field-effect transistors: Ambipolar transport characteristics. *Appl. Phys. Lett.* **84,** 2412–2414 (2004).

7. Hafner, J. H. *et al.* Catalytic growth of single-wall carbon nanotubes from metal particles. *Chem. Phys. Lett.* **296,** 195–202 (1998).
8. Flahaut, E., Peigney, A., Bacsa, W. S., Bacsa, R.R. & Laurent, Ch. CCVD synthesis of carbon nanotubes from (Mg,Co,Mo)O catalysts: influence of the proportions of cobalt and molybdenum. *J. Mater. Chem.* **14,** 646–653 (2004).
9. Li, W. Z., Wen, J. G., Sennett, M. & Ren, Z. F. Clean double-walled carbon nanotubes synthesized by CVD. *Chem. Phys. Lett.* **368,** 299–306 (2003).
10. Lyu, S. C. *et al.* Large-scale synthesis of high-quality double-walled carbon nanotubes by catalytic decomposition of *n*-hexane. *J. Phys. Chem. B* **108,** 2192–2194 (2004).
11. Cumings, J., Mickelson, W. & Zettl, A. Simplified synthesis of double-wall carbon nanotubes. *Solid State Commun.* **126,** 359–362 (2003).
12. Hiraoka, T. *et al.* Selective synthesis of double-wall carbon nanotubes by CCVD of acetylene using zeolite supports. *Chem. Phys. Lett.* **382,** 679–685 (2003).
13. Zhu, J., Yudasaka, M. & Iijima, S. A catalytic chemical vapor deposition synthesis of double-walled carbon nanotubes over metal catalysts supported on a mesoporous material. *Chem. Phys. Lett.* **380,** 496–502 (2003).
14. Ago, H., Nakamura, K., Uehara, N. & Tsuji, M. Roles of metal-support interaction in growth of single- and double-walled carbon nanotubes studied with diameter-controlled iron particles supported on MgO. *J. Phys. Chem. B* **108,** 18908–18915 (2004).
15. Lyu, S. C., Lee, T. J., Yang, C. W. & Lee, C. J. Synthesis and characterization of high-quality double-walled carbon nanotubes by catalytic decomposition of alcohol. *Chem. Commun.* 1404–1405 (2003).
16. Endo, M. *et al.* 'Buckypaper' from coaxial nanotubes. *Nature* **433,** 476 (2005).
17. Ramesh, P. *et al.* Purification and characterization of double-wall carbon nanotubes synthesized by catalytic chemical vapor deposition on mesoporous silica. *Chem. Phys. Lett.* **418,** 408–412 (2006).
18. Hutchison, J. L. *et al.* Double-walled carbon nanotubes fabricated by a hydrogen arc discharge method. *Carbon* **39,** 761–770 (2001).
19. Saito, Y., Nakahira, T. & Uemura, S. Growth conditions of double-walled carbon nanotubes in arc discharge. *J. Phys. Chem. B* **107,** 931–934 (2003).
20. Sugai, T. *et al.* New synthesis of high-quality double-walled carbon nanotubes by high-temperature pulsed arc discharge. *Nano Lett.* **3,** 769–773 (2003).
21. Bandow, S., Takizawa, M., Hirahara, K., Yudasaka, M. & Iijima, S. Raman scattering study of double-wall carbon nanotubes derived from the chains of fullerenes in single-wall carbon nanotubes. *Chem. Phys. Lett.* **337,** 48–54 (2001).
22. Ren, W. & Cheng, H. M. Aligned double-walled carbon nanotube long ropes with a narrow diameter distribution. *J. Phys. Chem. B* **109,** 7169–7173 (2005).
23. Wei, J., Jiang, B., Wu, D. & Wei, B. Large-scale synthesis of long double-walled carbon nanotubes. *J. Phys. Chem. B* **108,** 8844–8847 (2004).
24. Hata, K. *et al.* Water-assisted highly efficient synthesis of impurity-free single-walled carbon nanotubes. *Science* **306,** 1362–1364 (2004).
25. Futaba, D. N. *et al.* Kinetics of water-assisted single-walled carbon nanotube synthesis revealed by a time-evolution analysis. *Phys. Rev. Lett.* **95,** 056104 (2005).
26. Futaba, D. N. *et al.* 84% catalyst activity of water-assisted growth of single walled characterization by a statistical and macroscopic approach. *J. Phys. Chem. B* **110,** 8035–8038 (2006).
27. Huang, Z. P. *et al.* Effect of nickel, iron and cobalt on growth of aligned carbon nanotubes. *Appl. Phys. A* **74,** 387–391 (2002).
28. Wang, Y.Y., Gupta, S. & Nemanich, R. J. Role of thin Fe catalyst in the synthesis of double- and single-wall carbon nanotubes via microwave chemical vapor deposition. *Appl. Phys. Lett.* **85,** 2601–2603 (2004).
29. Wang, Y. Y., Gupta, S., Nemanich, R. J., Liu, Z. J. & Qin, L. C. Hollow to bamboolike internal structure transition observed in carbon nanotube films. *J. Appl. Phys.* **98,** 014312 (2005).
30. Futaba, D. N. *et al. Nature Mater.* (submitted).
31. Xu, Y. Q. *et al.* Vertical array growth of small diameter single-walled carbon nanotubes. *J. Am. Chem. Soc.* **128,** 6560–6561 (2006).
32. Holt, J. K. *et al.* Fast mass transport through sub-2-nanometer carbon nanotubes. *Science* **312,** 1034–1037 (2006).
33. Hongo, H. *et al.* Support materials based on converted aluminum films for chemical vapor deposition growth of single-wall carbon nanotubes. *Chem. Phys. Lett.* **380,** 158–164 (2003).
34. Seidel, R. *et al.* In-situ contacted single-walled carbon nanotubes and contact improvement by electroless deposition. *Nano Lett.* **3,** 965–968 (2003).
35. Zhang, R. Y., Amlani, I., Baker, J., Tresek, J. & Tsui, R. K. Chemical vapor deposition of single-walled carbon nanotubes using ultrathin Ni/Al film as catalyst. *Nano Lett.* **3,** 731–735 (2003).

Acknowledgements

We thank A. Maigne, T. Nakamura and Y. Kakudate for their helpful experimental support. We also gratefully acknowledge the helpful contributions by A. Otsuka, S. Yamada, M. Mizuno and T. Hiraoka. The partial support of the New Energy and Industrial Technology Development Organization (NEDO) Nano-Carbon Technology project is acknowledged.

Author contributions

T.Y. and K.H. conceived and designed the experiment, T.Y. and T.N. performed the experiments, K.M. contributed to material preparation, and J.F. and M.Y. contributed to TEM observations. T.Y. and K.H. co-wrote the paper.

Competing financial interests

The authors declare that they have no competing financial interests.